

Article ID 1004-924X(2007)12-1850-12

基于多层膜的软 X 射线偏振测量

Franz Schaefers

(BESSY, Berlin, Germany)

摘要:综述了过去 10 年中德国 BESSY 同步辐射装置在软 X 射线偏振测量方面所做的工作。在 BESSY 同步辐射装置中,有 10 条椭圆波荡器光束线,这可使同步加速器辐射的偏振态从线偏振光(水平或者垂直)转变为左旋或右旋圆偏振光。由于很多偏振敏感实验(例如, MCD 光谱测量)需要归一化量,因此对偏振度进行量化非常重要。对于偏振实验,即对光的偏振态测量来说,需要两个光学元件分别起相位片和检偏器作用。因此,专门研制了在软 X 射线区有透射和反射功能的多层膜,并对其做了优化。通过使多层膜参数(周期,厚度比)与构成材料的吸收边相匹配,即可获得共振加强的偏振灵敏度。由此可知,基于多层膜的偏振测量与这些偏振光学元件工作波长处性能测量密切相关,文中对仪器的设置和测试结果做了介绍,同时给出了磁性薄膜或光活化物质的磁光光谱测量和偏振测量的示例(法拉第和克尔效应)。

关键词:多层膜;软 X 射线;极紫外辐射;同步辐射;偏振测量;检偏器;相位片;反射率;磁光效应

中图分类号: O434.12 **文献标识码:** A

Multilayer-based soft X-ray polarimetry

Franz Schaefers

(BESSY, Berlin, Germany)

Abstract: An overview of the soft X-ray polarimetry undertaken at BESSY over the last 10 years is presented. At BESSY, ten elliptical undulator beamlines are operating in the VUV and soft X-ray range, which enables the polarisation state of the synchrotron radiation to be changed from linear (horizontal or vertical) to left- or right-handed circular. It is essential that the degree of polarisation is known quantitatively, since this is a normalization quantity for many polarisation-sensitive experiments (*e. g.* MCD-spectroscopy).

For a polarimetry experiment *i. e.* the measurement of the polarisation state of light, two optical elements are required acting as a phase retarder and a linear polariser, respectively. In the soft X-ray range, specially tailored multilayers (ML) operating in transmission and in reflection have been developed and optimized for this purpose. By matching the ML-parameters (period, thickness ratio) to an absorption edge of one of the constituent materials, a resonantly enhanced polarisation sensitivity can be achieved. Thus, ML-polarimetry is strongly connected with At-Wavelength Metrology of these polarisation optical elements, for which the instrumentation and results are presented. Examples of magneto-optical spectroscopy and polarimetry to determine properties of magnetic thin films or optically active substances are also presented (Faraday and Kerr effect, L-MOKE).

Key words: multilayer; soft X-ray radiation; EUV radiation; synchrotron radiation; polarimetry; linear analyser; phase plate; reflectivity; magneto-optic instrument

1 Introduction

Studies of magnetic scattering^[1-4] and magneto-optics^[5-9] using synchrotron radiation require knowledge of the beam polarization, which is also necessary to characterize EUV optical elements at off-normal incidence angles^[10-13]. The ability to analyze the polarization state of the beam is of practical importance in evaluating the performance of insertion-device synchrotron sources^[14]. Experimental control and evaluation of a beam's polarization state can be obtained with optical devices such as phase retarders and linear analyzers^[15-17]. Periodic MLs are commonly used to study the polarization state of EUV and VUV beams^[18-21], which must be changed or rotated to perform polarization analyses because of their intrinsically narrow wavelength acceptance. This paper reviews the polarimetry work performed at BESSY, the German storage ring facility, during the last two decades.

BESSY operates a medium energy 1.7 GeV storage ring with 16 straight sections of which ten are occupied by soft X-ray undulators, six of them are elliptical APPLE II-devices for the generation of polarised light. More than 40 beamlines are operational from the IR to hard X-rays with special emphasis on the soft X-ray range. Each of the undulators branches the light into two or more beamlines which are used alternatively. Thus fourteen undulator beamlines and additionally two polarised bending magnet beamlines exploiting the off-plane radiation are dedicated to polarisation sensitive experiments in the EUV, VUV and soft X-ray range^[22]. All these beamlines had to be characterised with respect to their polarisation properties.

In section 2 the development and characteri-

sation of special ML-optics for polarisation control and steering by the At-Wavelength Metrology is discussed. This is a prerequisite for polarisation spectroscopy. Then the ML-polarimetry will be dealt with in section 3. In section 4 some examples of polarisation spectroscopy are given; a spin-off from the technique of ML-polarimetry.

2 At-Wavelength Metrology

At-Wavelength Metrology is the measure of the performance of an optical element at the wavelength, for which it is designed. Apart from routine tests employing Cu-K α diffractometry which delivers information on interfacial roughness and the quality of the coated reflecting layers, and apart from long-trace profilometry which delivers information on the figure and finish errors of optical surfaces, At-Wavelength Metrology is the most powerful and most essential characterisation tool for the development and characterisation of soft X-ray optics, since optical properties such as reflectivity are governed by the optical properties of the materials involved which are strongly dependent on wavelength.

An example for the necessity of At-Wavelength Metrology as a 'test drive' is shown in Fig. 1^[23-24]. This is the reflectivity curve of a Sc/Si ML, which has a normal-incidence Bragg reflection at 45 nm in the UV-region. The ML with a period thickness of 22.5 nm has only 10 periods, nevertheless it has an extraordinary reflectivity of 50 %. The Sc curve is obtained by a second ML with vanishing reflectivity.

The important point here is that the ML are nearly identical; they have been sputtered one after the other in the same chamber under the same conditions. The only difference between

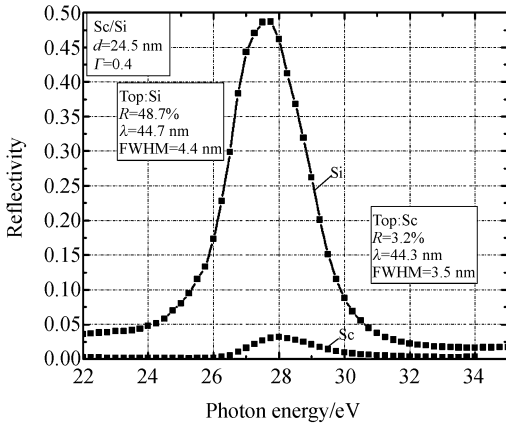


Fig. 1 Comparison of two similar Sc/Si multilayers with Si and Sc top layer coating measured 'at wavelength'

them is the outermost layer which is either silicon or scandium. A Cu-K α test gives no difference in their performance, which means that their quality, periodicity and interface perfection are similar, as expected. Such a dramatic effect can be detected only at the design wavelength.

The UV-region is known to be highly absorbing, in other words the penetration depth of the light is rather limited. Thus an optical element is contamination and surface-sensitive, because radiation is absorbed in the outermost layer. It is therefore surprising that a ML can show such a response. This is due to the anomalous optical features of the Sc absorber material^[25]. Sc as the first element of the 3d-transition metals with electronic configuration 3p⁶3d4s² has a nearly empty d-shell with just one electron. The 3p-3d electronic transition occurs in the UV-range. Since the d-shell of Sc is nearly unoccupied, Sc has the largest oscillator strength of all transition metals associated with the largest absorption.

This is connected with an absorption minimum just below the transition which again is most pronounced for Sc. So Sc has the potential of being a good ML absorber material, exclusively in this range. The deeper the absorption minimum, the larger is the penetration depth of

light, and the larger the penetration depth, the more layers contribute to the reflection and, consequently, the larger the reflectance as can be seen in Fig. 2, where the reflectivity of different Sc/Si ML is plotted. Their period was varied systematically to ensure that the Bragg-maximum is always at the same angle of 5° to normal.

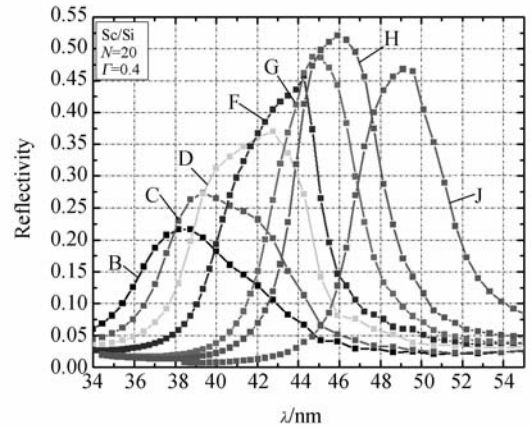


Fig. 2 Normal-incidence reflectivity ($\theta=85^\circ$) of Sc/Si multilayers with different periods measured in the UV range

It is interesting to note that at the wavelength of maximum performance, 46.9 nm, a powerful table-top X-ray laser line operates^[26].

The working range of ML operation in the VUV range is limited to the vicinity of the absorption edges of one of the constituent materials. A resonantly-enhanced performance increase is thus present at the Si-, B-, and C-K edges and for the water-window range at the 2p edges of the rare earth elements. However, performance degrades with increasing photon energy, because the material contrast determined by the optical constants decreases rapidly and the influence of roughness increases with energy, since the layers approach monolayer thickness.

At BESSY, a soft X-ray optics beamline for metrology^[27] is operational and is coupled to a bending magnet that is equipped with a reflectometer endstation (Fig. 3).

This is a collimated plane grating mono-

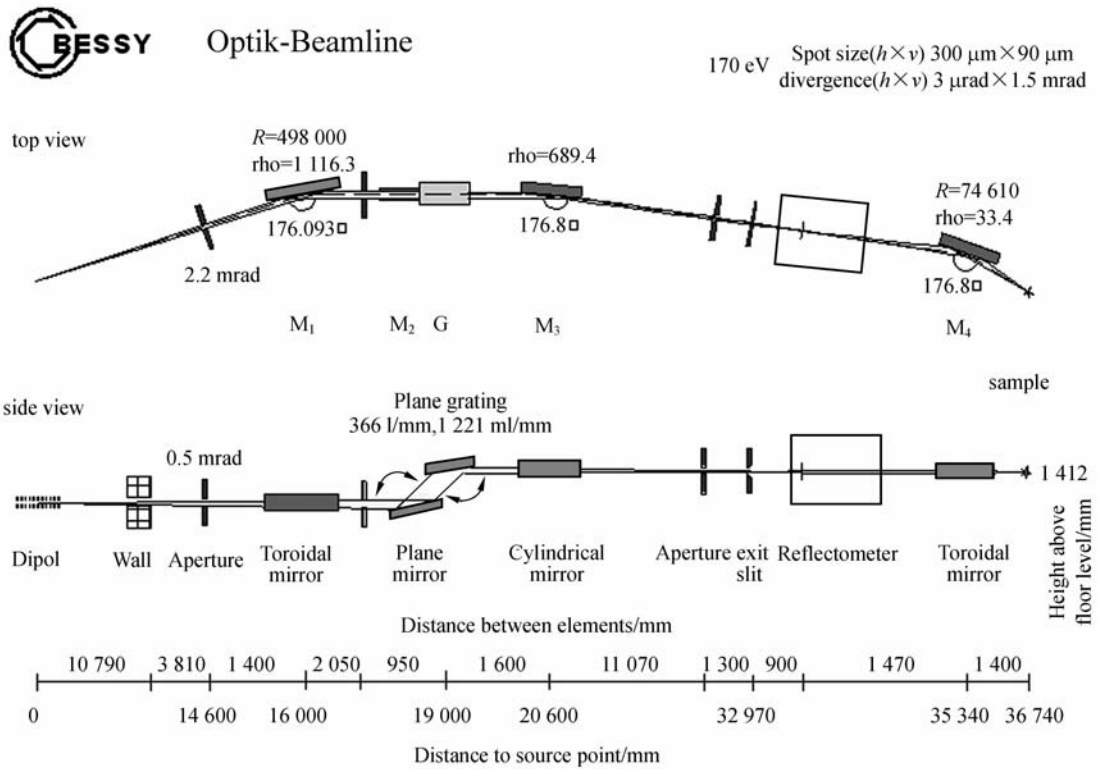


Fig. 3 BESSY soft X-ray optics beamline for At Wavelength Metrology of optical components employing a plane grating monochromator in collimated light

chromator operating from 20 to 1 500 eV. It can be tuned to linear or (off-plane) elliptical polarisation. By operating the grating using collimated light^[28] it has flexibility in the operation modes, such as high-order suppression, that is essential for reflectometry.

The most prominent ML for the water window is Cr/Sc for operation at either the Sc or Cr 2p absorption edges. Their evolution and improvement has been studied over the last decade^[29-30]. As shown in Fig. 4, we developed two types of reflectors for the Sc-near edge region: Brewster angle mirrors for polarimetry purposes operating close to 45° incidence angle and normal incidence mirrors for water-window microscopy and N-K fluorescence analysis applications. The reflectivity could be increased by more than a factor of two in both cases and a 20% normal incidence reflectivity at 400 eV within a 1 eV bandwidth is available today^[31]. Such a high-tech mirror requires a sophisticated layer-by-layer

production and atomic scale interface engineering, accompanied by ion assisted deposition. An angular scan providing a depth profile of the ML confirms the high individual layer conformity.

A survey of all the individual reflection data collected over the years is given in the Fig. 5. Plotted is the peak reflectivity in normal incidence. Each data point corresponds to one individual ML. The resonance behaviour of the reflectivity is clearly seen at all the absorption edges up to the Ti and V 2p-edges above 500 eV which seems to be the practical limit for normal incidence spectroscopy. A similar figure can be constructed for the case of Brewster-angle polarisers operating at 45°. Since the ML-period in this case is larger by a factor of $1/\sin(45^\circ)$ for the same photon energy, polarisers are available at the 2p edges of the magnetic elements Fe, Co and Ni where most of the polarisation spectroscopy is being performed.

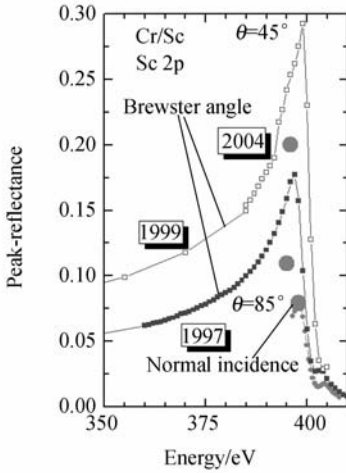


Fig. 4 Evolution of Cr/Sc reflectivity in the water window during the last decade. Normal incidence and Brewster angle

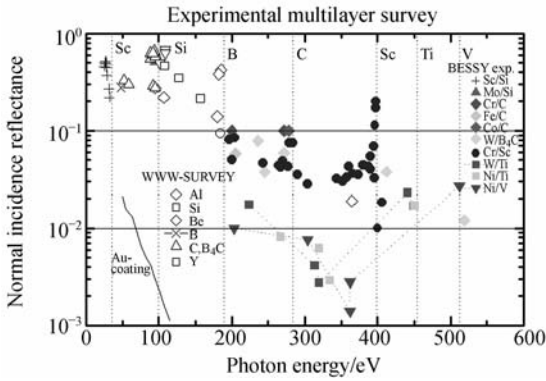


Fig. 5 Experimental multilayer survey for the UV, EUV and soft X-ray range. Normal incidence reflectivity is shown only ($\theta > 80^\circ$)

3 Multilayer polarimetry

Multilayer polarimetry is a spin-off from At Wavelength Metrology. The detailed knowledge of the polarisation properties of MLs is a prerequisite to its application to the measurement of the complete polarisation state of synchrotron radiation. This follows standard optics textbooks by employing two optical elements which are azimuthally rotated around the direction of the light, a polariser to introduce a phase retardation and an analyser for linear polarisation analysis^[32].

An ideal polariser retards the phase by a quarter of a wavelength, and does not affect the amplitude, while an ideal analyser suppresses one component completely and does not affect the phase.

Any interaction of the optics with the electromagnetic wave is represented by the complex reflection (or transmission) coefficients r_s or r_p , where

$$E_s' = r_s E_s, \quad E_p' = r_p E_p. \quad (1)$$

The polarisation is described by the Stokes vector, for intensity S_0 , linear polarisations S_1 and S_2 and circular polarisation S_3 . The interaction process is described by the Müller matrix

$$M = \begin{bmatrix} 1 & -\cos 2\Psi & 0 & 0 \\ -\cos 2\Psi & 1 & 0 & 0 \\ 0 & 0 & \sin 2\Psi \cos \Delta & \sin 2\Psi \sin \Delta \\ 0 & 0 & -\sin 2\Psi \sin \Delta & \sin 2\Psi \cos \Delta \end{bmatrix}, \quad (2)$$

which is basically determined by the two parameters of ellipticity Ψ and total phase retardation Δ to describe the complex reflection or transmission coefficient.

$$\begin{aligned} \Psi &= a \tan(r_p/r_s) \\ \Delta &= \delta_p - \delta_s \end{aligned} \quad (3)$$

For our two-optical element polarimeter system the Stokes vector at the detector, S_{final} , is obtained by the initial Stokes vector of the incoming light, multiplied by the rotation-matrix, Müller-matrix and back rotation matrix of the first optical element (rotated by α), and similarly for the second optical element which is rotated by β ^[33]:

$$S_{\text{final}} = R(-\beta) M_2 R(\beta) R(-\alpha) M_1 R(\alpha) S_{\text{initial}}. \quad (4)$$

The detector sees a 3-D intensity contour, such as that in Fig. 6 as function of α and β when we assume an ideal polarimeter and circularly polarised incident light ($S_3 = 1$ Fig. 6(a)) and linearly polarised light Fig. 6(b), respectively.

A fit of the experimental data to this contour determines not only the Stokes parameters of the incident light, but also the polarising properties of the optical elements involved such

as R_s/R_p , T_s/T_p and the phase shift Δ . Thus this is a self-calibrating measurement as one does not need to know details about the optics, the measurement itself gives all relevant data. This requires, however, a redundancy in the number of measured data and high quality datum points for the fitting procedure to converge properly.

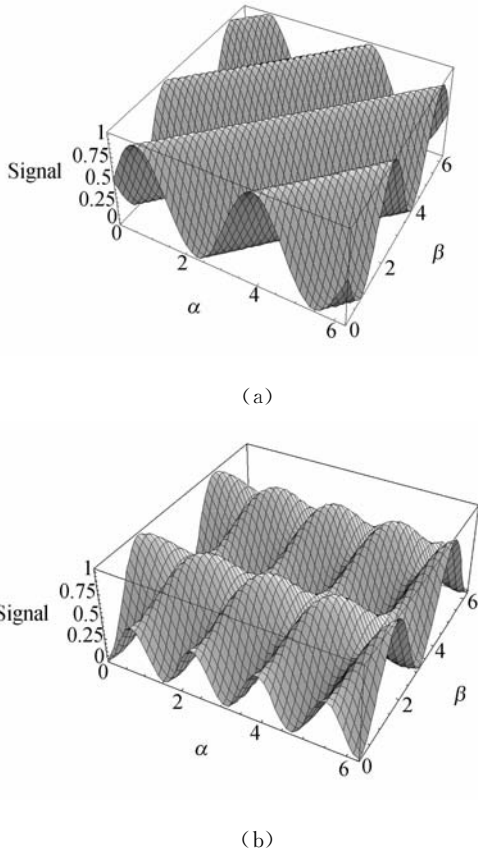


Fig. 6 Calculated polarimeter signal for circularly (a) and linearly polarised (b) light assuming an ideal polarimeter optics ($T_s = T_p, \Delta = 90^\circ, R_p = 0$)

Linear analysers and phase plates are common for the visible, and UV spectral range. In EUV, triple- and quadruple-reflection mirrors have been designed with incidence angles for optimum phase retardation or analyser behaviour^[34-35]. For the soft X-ray range specially tailored, MLs operating in reflection and transmission have been developed in the last decade^[36]. Similar to the MLs optimised for highest reflec-

tion, the phase retardation obtainable with transmission MLs is resonantly enhanced at the absorption edges, thus the tuning range is limited, and the phase shift dies away with higher energies due to roughness and lack of contrast in the optical constants.

Several type of apparatus for full polarisation measurements in the soft X-ray range have been reported^[37]. The BESSY soft X-ray polarimeter^[20] shown in Fig. 7 is able to perform such a polarisation measurement according. In this 6-axis UHV-diffractometer the light hits a polariser and analyser section, both azimuthally rotatable, and the incidence angle is freely changeable. The detector is scanning both in the dispersion plane and perpendicular to it.

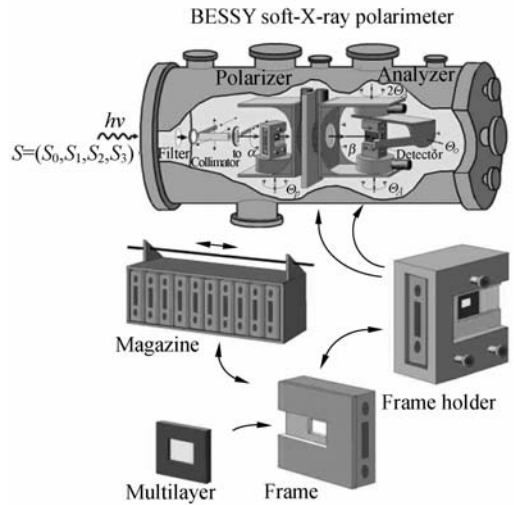


Fig. 7 BESSY soft X-ray UHV-compatible 6 axis polarimeter

Up to ten optical elements are selectable from a magazine store in vacuum. Additionally a load-lock system enables rapid sample transfer from air to UHV within half an hour.

This versatility allows the chamber to be used not only as a polarimeter for incident light spectroscopy. When one of the optics is removed, it becomes a reflectometer for intensity spectroscopy in transmission or reflection geometry. Transmission optics ellipsometry can also be undertaken, since not only the transmitted intensity but also the polarisation state after

transmission can be studied. The photo in Fig. 8 shows a compact version of the polarimeter in use at BESSY^[38]. This one was designed for in-situ control of the polarisation state in various elliptical undulator beamlines. All optical parts are removeable, so, it can be permanently coupled between the beamline and an experiment.

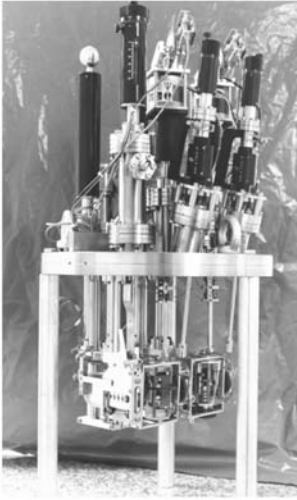


Fig. 8 BESSY compact polarimeter for in-situ control of polarisation with removable optics

Fig. 9 shows the reflectivity of a Cr/Sc ML for s- and p-polarised light^[29]. The period was exactly matched, so that the Bragg-peak coincides with the Brewster angle at 45° at the design energy, which is close to the Cr 2p edge. The suppression ratio r_s/r_p is more than 1 000, thus the polarizing power more than 99.8%. By such a matching of both polarizing angle and resonance energy the excellent polarizing power is combined with high reflectivity. An azimuthal scan of the polariser around the light direction from 0° to 360° confirms this behaviour (Fig. 10). In normal incidence geometry, however, no angular dependence is observed, as expected. Note, that this ML can be operated in two working ranges; at the Cr edge at 45° as an analyser and at the Sc edge as a highly efficient normal incidence reflector.

Transmission ML-phase plates are sputtered on 120 nm thick Si_3N_4 membranes. The Bragg

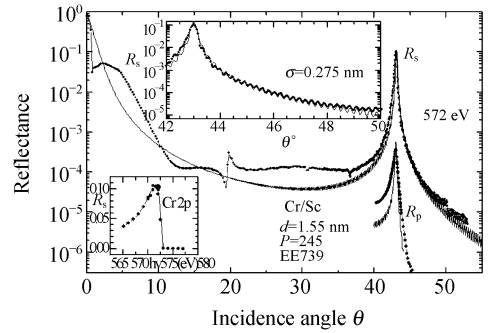


Fig. 9 Reflectivity of Cr/Sc ML for s- and p-polarised light at 572 eV, right below the Cr 2p absorption edge (see inset). The range of the Brewster angle is enlarged in the inset.

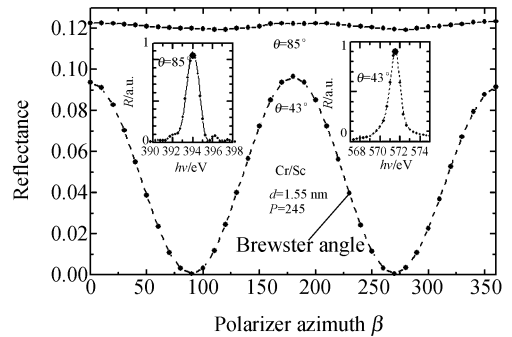


Fig. 10 Polarimeter scans at the Brewster angle and in normal incidence, respectively. The energies correspond to Cr and Sc absorption edges, respectively (see inset).

reflection resonance at a certain photon energy manifests itself as transmission minimum at the Bragg-angle. As seen in Fig. 11 this minimum is resonantly enhanced in the region of the absorption edge - here the Sc 2p edge - and it is connected with a large phase retardation as a function of the angle in the vicinity of the Bragg-angle (Fig. 12).

The measured 30° phase shift at 400 eV is still far away from a quarter-wave behaviour, but this is sufficient for a unique determination of the polarisation state by the fitting procedure explained above.

A survey of the phase shift data available by ML is summarised as follows. For the UV-range, MgF_2 optics has been added to this sur-

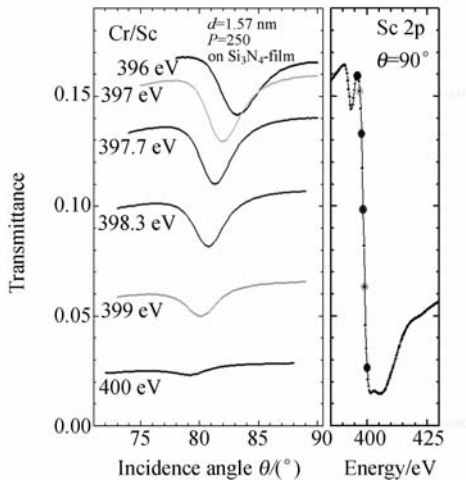


Fig. 11 Transmission of a Cr/Sc ML on a SiN membrane in the vicinity of the Sc 2p resonance.

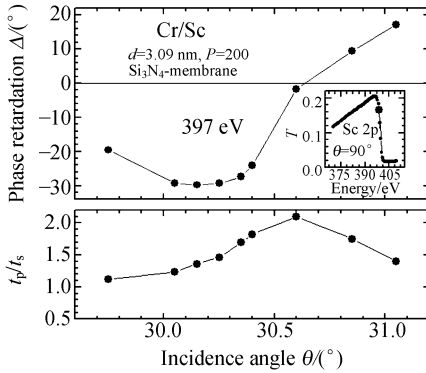


Fig. 12 Corresponding phase retardation through the Bragg transmission minimum.

vey and at the Si L edge (100 eV) there is a quarter-wave plate of Mo/Si^[18-19]. In the water window range four systems were developed for the C edge and the Sc, Ti and Cr edges. As expected, the performance is strongly dependent on the material combination and it decreases at higher photon energies. Recently a broad-band Mo/Si ML was reported^[39-40], which is tuneable in wavelength within a bandwidth of approximately 10%. This was realised by a random modification of the individual layer thicknesses to make the rocking curve broader, but at the price of reduced reflectivity and phase shift.

At the Sc edge a quarter-wave plate was reported recently^[21,41] employing high quality Cr/Sc MLs with individual thicknesses in the range

of 1 nm. Due to the necessity for ultra-short period the practical limit for this technology has been almost reached at these energies.

While linear polarisation analysers with sufficient accuracy are available at even higher energy^[42], it may be worthwhile developing phase plates for the magnetic Fe, Co and Ni 2p edges which require some hundred periods with layer thicknesses as small as 0.5 nm. Most of the polarisation spectroscopy work is undertaken here and no polarisation determination employing optical standards is possible so far. The degree of circular polarisation can be estimated only by transfer standards (such as MCD-detectors^[43]) which need to be calibrated once against a linear polarisation standard under the assumption of complete total polarisation without any unpolarised background radiation.

4 Magneto-optics

Magneto-optics deals with the interaction of radiation with magnetic materials; the optical response to magnetised matter. In analogy to non-magnetic optics this response is put into magneto-optical constants of the form

$$n_{\pm} = 1 - (\delta_1 \pm \Delta\delta) + i(\beta_1 \pm \Delta\beta), \quad (5)$$

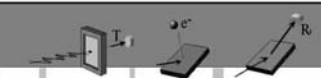
with δ_1 and β_1 being the non-magnetic optical constants, and $\Delta\delta$ and $\Delta\beta$ the 'magnetic perturbation' of the optical interaction^[44]. The positive and negative signs denote the orientation of the magnetic field with respect to the polarisation direction. The difference $\Delta n = n_+ - n_-$ denotes the circular dichroism of the material. Similar to the optical interaction, the magneto-optical properties are resonantly enhanced at the absorption edges of the magnetic sub-states, such as the L-, or M-edges of Fe, Co and Ni.

In the BESSY located chamber (Fig. 7) samples can be magnetised in-situ by in-vacuum magnetic coils located around the sample holder, and an iron yoke close to the sample surface, which directs the magnetic flux through the

sample. Two magnetisation directions can be realised for both the reflection and transmission sample; in-plane in two directions (reflection) and out-of plane (transmission sample). Nevertheless, the full versatility and flexibility in angle settings and in-situ sample change is kept, so that a variety of different measurement techniques can be established, which makes use of many degrees of freedom;

- * incident radiation; energy, polarisation
- * magnetization direction (in-plane, out-of plane)
- * orientation of both light (k -vector and spin) and magnetization; parallel, longitudinal, transverse
- * azimuth and incidence angle
- * detection channel (intensity, polarisation)

Fig. 13 gives an overview about this array of experimental possibilities connected with magneto-optical effects^[45]. They can first be classified according to the detection channel, whether the intensity or the polarisation of the scattered light is being investigated after the interaction process. The magnetic sensitivity is either linear or quadratic with the magnetic field. A linear effect in M changes sign on magnetisation reversal, an odd effect does not.



Detection	Magnetic sensitivity	Light-pola.	Transmission	Absorption	Reflection
Intensity measurement	$\langle M \rangle$	circ. lin.	XMCD	—	XRMS T-MOKE
	$\langle M^2 \rangle$	lin.	XMLD		XMLD-type Reflectometry
Polarization analysis	$\langle M \rangle$	lin.	Faraday		Kerr L-P-MOKE
	$\langle M^2 \rangle$	lin.	Voigt		

Fig. 13 Summary of magneto-optical effects and their measurement

Some effects are proportional to the degree of circular polarisation, others to the degree of linear polarisation, while the other Stokes com-

ponent in this case is ineffective.

For example, the classical MCD probes the spin-up and spin-down bands, so it is measurable with circularly polarised light and the magnetic contrast, while the asymmetry is obtained by reversing the orientation (parallel - antiparallel) between the magnetization direction and photon helicity. The linear dichroism is measured in a different geometry, since it is an M^2 effect. The contrast is given by parallel and perpendicular orientation between the electric field vector and magnetization.

Polarisation spectroscopy with MLs enables the classical Faraday effect (transmitting samples) and Kerr effect - L-MOKE (in reflection) to be measured resonantly, enhanced by tuning the photon energy to the 2p-absorption edges in the soft X-ray range. These effects are linear in M and change sign on M -reversal and also have the advantage that their measurement requires only linearly polarised light only, which usually is easier to obtain rather than circular polarisation.

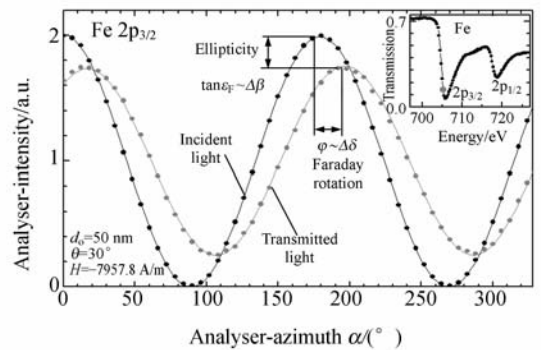


Fig. 14 Ellipsometry on magnetic Fe: Faraday effect on a thin Fe film measured with linearly polarised light resonantly enhanced within the Fe 2p absorption edge (see inset)

An example of the measurement of the Faraday effect is given in Fig. 14^[46-47]. Here a polarisation measurement of the incident light (Incident light curve) and the light after transmission through a magnetised Fe-film (Transmitted light curve) is shown. After transmission, the polari-

sation plane is tilted and ellipticity is induced. Both ellipsometric parameters ϕ and $\tan \epsilon$ can be traced back to the magneto-optical quantities $\Delta\delta$ and $\Delta\beta$. The Faraday-rotation angles are 100 times larger than those measured in the visible, when it is measured element-specific and resonantly enhanced within the 2p-absorption edge. Such a thin magnetic film can be used for steering the linear polarisation plane and to rotate the e -vector by up to 90° , the angle being determined by the thickness of the film. Though the Faraday-effect is measured with linearly polarised light, dichroism can be sampled with this technique, since the linear polarisation can be thought of being composed of two circular polarised waves of equal intensity but opposite helicity, for which the absorption is different due to the circular dichroism of the system.

For polarisation spectroscopy to be established as a tool for magnetic materials research, the transmission geometry is of rather limited use, since most samples cannot be produced ultra-thin films of less than a nanometer thickness in order to have a significant transmitted signal. The analogue to the Faraday-effect in reflection is called the Kerr-effect, *i. e.* the polarisation analysis of the light reflected by a magnetic sample. By a miniaturised polarisation detector sitting on the detector holder, such a measurement is possible using the BESSY polarimeter.

Fig. 15 shows an example for the Kerr-effect measured on a Co sample using linearly polarised light^[48]. The reflectivity and the change of polarisation in terms of the rotation angle ϕ and ellipticity $\tan \epsilon$ were measured across the Co 2p absorption. Both data are used for determination of the magneto-optical constants according to:

$$\begin{aligned} \text{Rotation } \theta_s &= \frac{\Delta\delta(\beta_1 - \beta_0) - \Delta\beta(\delta_0 - \delta_1)}{(\delta_0 - \delta_1)^2 - (\beta_1 - \beta_0)^2} \\ \text{Ellipticity } \epsilon_s &= \frac{\Delta\delta(\delta_0 - \delta_1) - \Delta\beta(\beta_1 - \beta_0)}{(\delta_0 - \delta_1)^2 - (\beta_1 - \beta_0)^2}, \end{aligned} \quad (6)$$

The indexes 0 and 1 correspond to vacuum

level (or a non-magnetic top-layer) and to the non-magnetic part of the refractive index (see Eq. 5), respectively. The agreement with data obtained by other methods like MCD and resonant Bragg-reflection is good.

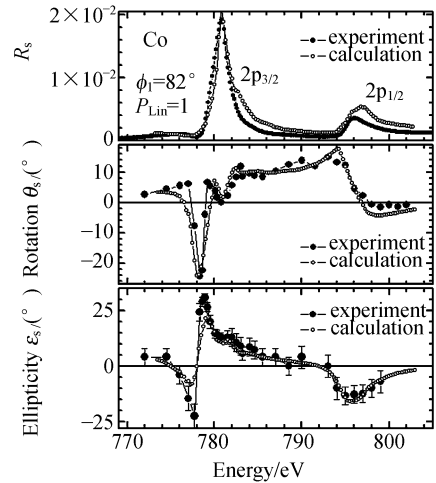


Fig. 15 Ellipsometry on magnetic Co: Kerr effect on a thin Co film measured with linearly polarised light resonantly enhanced across the Co 2p absorption edge

This technique of polarisation spectroscopy which is just soft X-ray ellipsometry is not restricted to magnetic samples and magnetic dichroism. All optically active samples which have intrinsically any kind of anisotropy can be addressed element-specifically. Fig. 16 shows the experimental data for a graphitic sample^[49]. Graphite has a hexagonal crystal structure, and this structural anisotropy leads to a natural linear dichroism. It is strongly birefringent at the carbon K-edge. The incident linear polarisation is resonantly modified within the absorption resonance. The polarisation plane is rotated by up to 90° and also circular polarisation is induced. Such a behaviour has serious consequences for optical elements inside a synchrotron radiation beamline, where, typically, carbon contamination is encountered due to the heat loading on the mirror surfaces. Regardless of the chemical composition of the carbon layer the beamline will be

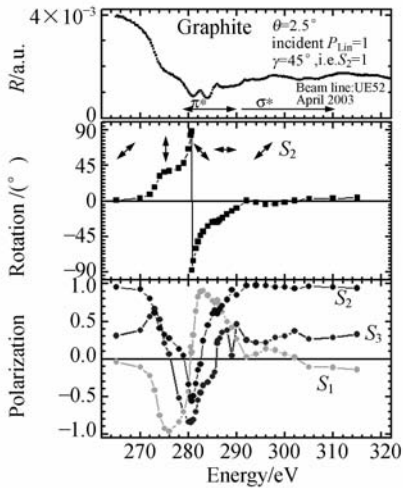


Fig. 16 Ellipsometry on a dichroic graphitic C; Kerr effect on a hexagonal graphite crystal measured with linearly polarised light resonantly enhanced across the C 1s absorption edge

optically active. Not only does the photon flux drop at the carbon edge, but the polarisation changes dramatically! Thus polarisation sensitive experiments at the carbon edge need careful monitoring of the polarisation stage.

5 Conclusions

The interaction of polarised soft X-ray radiation with matter can best be studied by polarisation spectroscopy. This allows for the deter-

References:

- [1] HECKER M, VALENCIA S, OPPENEER P M, *et al.* [J]. *Phys. Rev. B*, 2005, 72:054437-054442.
- [2] KORTRIGHT J B, AWSCHALOM D D, STÖHR J, *et al.* [J]. *Magn. Magn. Mater*, 1999, 207:7.
- [3] KORTRIGHT J B, KIM S K. [J]. *Phys. Rev. B*, 2000, 62:12216-12228.
- [4] DUERR H A, DUDZIK E, DHESI S S, *et al.* [J]. *Science*, 1999, 284:2166-2168.
- [5] KAO C C, CHEN C T, JOHNSON E D, *et al.* [J]. *Phys. Rev. B*, 1994, 50:9599-9602.
- [6] GEISSLER J, GOERING E, JUSTEN M, *et al.* [J]. *Phys. Rev. B*, 2001, 65:020405-020408.
- [7] SACCHI M, MIRONE A. [J]. *Phys. Rev. B*, 1998, 57:8408-8415.
- [8] MERTINS H C, OPPENEER P M, KUNES J, *et al.* [J]. *Phys. Rev. Lett.* ,2001, 87:047401-047404.
- [9] MERTINS H C, ABRAMSOHN D, GAUPP A, *et al.* [J]. *Phys. Rev. B*, 2002, 66:184404-184411.
- [10] SCHAEFERS F. [J]. *Physica B*, 2000, 283:119-124.
- [11] ANDREEV S S, AKHSAKHALYAN A D, BIBISHKIN M A, *et al.* [J]. *CEJP*, 2003, 1:191-209.
- [12] GRIMMER H, BÖNI P, BREITMEIER U, *et al.* [J]. *Thin Solid Films*, 1998, 319:73-77.
- [13] MONTCOLM C, KEARNEY P A, SLAUGHTER J M, *et al.* [J]. *Appl. Optics*, 1996, 35:5134-5147.
- [14] WEISS M R, FOLLATH R, SAWHNEY K J S, *et al.* [J]. *Nucl. Instrum. Meth. in Phys. Res. A*, 2001, 467-

mination of the complex optical constants.

By selecting the photon energy, this technique is element specific and by tuning the incidence angle it is depth selective.

It is also suited for the investigation of *e. g.* optically active substances - by which a symmetry break in the reaction geometry is induced by any kind of anisotropy such as natural birefringence or magnetic-field induced dichroism.

To measure all these effects requires polarisation sensitive optical elements for polarisation steering and control. They work best when resonantly enhanced at their respective absorption edges. Therefore an indispensable tool for their characterisation and development is At-Wavelength Metrology.

6 Acknowledgement

Hans-Christoph Mertins, Andreas Gaupp and Dirk Abramoohn are thanked for assisting in most of the work presented here. We thank all ML-suppliers from all over the world who kindly delivered most samples in-kind in exchange of characterization data.

468;449-452.

- [15] KLEIN M V, FURTAK T E. *Optik, Springer-Lehrbuch* [M]. Springer, 1988.
- [16] BORN M, WOLF E. *Principles of Optics* [M]. 6 th ed. Pergamon Press, 1980.
- [17] JENKINS F A, WHITE H E. *Fundamentals of Optics: IV* [M]. McGraw-Hill, 1981.
- [18] KORTRIGHT J B, UNDERWOOD J H. [J]. *Nucl. Instrum. Meth. A*, 1990, 291:272-277.
- [19] KORTRIGHT J B. [J]. *SPIE*, 1993, 2010:160-167.
- [20] SCHAEFERS F, MERTINS H C, GAUPP A, *et al.* [J]. *Applied Optics*, 1999, 38:4074-4088.
- [21] KIMURA H, HIRONO T, TAMENORI Y, *et al.* [J]. *Electron Spectr. and Relat. Phenom*, 2005, 144-147:1079-1091.
- [22] BAHRDT J, FENTRUP W, GAUPP A, *et al.* [J]. *Nucl. Instrum. Methods A*, 2001, 467-468:21-29.
- [23] SCHAEFERS F, YULIN S, FEIGL T, *et al.* [J]. *SPIE*, 2003, 5188:138-145.
- [24] YULIN S, SCHAEFERS F, FEIGL T, *et al.* [J]. *SPIE*, 2003, 5193:155-163.
- [25] VINOGRADOV A V. [J]. *Quantum Electronics*, 2002, 32:1113-1121.
- [26] BENWARE B R, MACCHIETTO C D, MORENO C H, *et al.* [J]. *Phys. Rev. Lett.*, 1998, 81:5804.
- [27] http://www.bessy.de/users_info/02.beamlines/
- [28] FOLLATH R. [J]. *Nucl. Instrum. and Methods A*, 2001, 467:418-425.
- [29] SCHAEFERS F, MERTINS H CH, SCHMOLLA F, *et al.* [J]. *Applied Optics*, 1998, 37:719-728.
- [30] SCHAEFERS F, MERTIN M, ABRAMSOHN D, *et al.* [J]. *Nucl. Instrum. Meth. in Phys. Res. A*, 2001, 467-8:349-353.
- [31] BIRCH J, ERIKSSON F, SCHAEFERS F, *et al.* [J]. *Applied Optics*, (submitted), 2005.
- [32] WESTERVELD W B, BECKER K, ZETNER P W, *et al.* [J]. *Appl. Opt.*, 1985, 24:2256-2262.
- [33] GAUPP A, MAST M. [J]. *Rev. Sci. Instrum.*, 2989, 60:2213-2215.
- [34] GAUPP A, PEATMAN W. [J]. *SPIE*, 1986, 733:272-273.
- [35] NAHON L, ALCARAZ C. [J]. *Appl. Opt.*, 2004, 43:1024-37.
- [36] GRIMMER H, ZAHARKO O, MERTINS H CH, *et al.* [J]. *Nucl. Instrum. Meth. in Phys. Res. A*, 2001, 467-8:354-357.
- [37] KIMURA H, HIRONO T, MIYAHARA T, *et al.* [C]. *Proc. SRI AIP*, 2004:537-540.
- [38] MERTINS H CH, SCHAEFERS F, ABRAMSOHN D, *et al.* [R]. *BESSY Annual Report*, 2000:342-343.
- [39] WANG Z, WANG H, ZHU J, *et al.* [J]. *Appl. Phys. Lett.*, 2007, 90(3):031901.
- [40] WANG Z, WANG H, ZHANG Z, *et al.* [J]. *Appl. Phys. Lett.*, 2007. (in press)
- [41] HIRONO T, KIMURA H, MURO T, *et al.* [J]. *J Electr. Spectrosc. and Relat. Phenom.*, 2005, 144-147:1097-1099.
- [42] GAUPP A, SCHAEFERS F, BRAUN S. [R]. *BESSY Annual Report*, 2005:449-450.
- [43] HOLLDAK K, SCHAEFERS F, KACHEL T, *et al.* [J]. *Rev. Sci. Instrum.*, 1996, 67:2485.
- [44] OPPENEER P M, BUSCHOW K H J. [J]. *Handbook of Magnetic Materials*, 2001, 13:229-422.
- [45] MERTINS H CH, VALENCIA S, GAUPP A, *et al.* [J]. *Appl. Phys. A*, 2005, 80:1011-1020.
- [46] MERTINS H CH, SCHAEFERS F, LECANN X, *et al.* [J]. *Phys. Rev. B*, 2000, 61:R874-R877.
- [47] KORTRIGHT J B, KIM S K. [J]. *Phys. Rev B*, 2000, 62:12216-12228.
- [48] MERTINS H CH, VALENCIA S, ABRAMSOHN D, *et al.* [J]. *Phys. Rev. B*, 2004, 69:064407-064412.
- [49] MERTINS H CH, OPPENEER P M, VALENCIA S, *et al.* [J]. *Phys. Rev. B*, 2004, 70:235106-235113.

Author's biography: Franz Schaefers, born in 1953 received his Physics Diploma in 1978 in radiation biology and his PhD in 1981 in atomic physics at the University of Muenster, Germany in 1981. Then he joined the surface physics departement of the Fritz-Haber Institute of the Max-Planck Society in Berlin. Since 1984 he is Senior Scientist at the BESSY GmbH, Berlin. He is engaged in X-ray optics and technology: synchrotron radiation beamline design and instrumentation and in the development and characterisation of X-ray (polarisation-) optical elements such as multilayers, mirrors, gratings and crystals. His special interests are development of raytracing software, polarimetry and reflectometry with multilayers. He is author of more than 100 publications in the above mentioned fields. E-mail:schaefers@bessy.de